MVACS Robotic Arm

Robert G. Bonitz, Jeffrey T. Slostad, Bruce Bon, Dave Braun, Russ Brill, Carl Buck, Richard Fleischner, Albert Haldeman, Jennifer Herman, Mark Hetzel, Don Noon, Greg Pixler, Paul Schenker, Thieu Ton, Curtis Tucker, and Wayne Zimmerman,

Jet Propulsion Laboratory

California Institute of Technology

4800 Oak Grove Drive

Pasadena, CA 91109-8099

Dave Paige

Department of Earth and Space Sciences

University of California at Los Angeles

595 Charles E. Young Drive East, Box 951567

Los Angeles, CA 90095

Abstract

The primary purpose of the Mars Volatiles And Climate Surveyor (MVACS) Robotic Arm is to support to the other MVACS science instruments by digging trenches in the Martian soil; acquiring and dumping soil samples into the Thermal Evolved Gas Analyzer (TEGA); positioning the Soil Temperature Probe (STP) in the soil: positioning the Robotic Arm Air Temperature Sensor (RAATS) at various heights above the surface, and positioning the Robotic Arm Camera (RAC) for taking images of the surface, trench, soil samples, magnetic targets and other objects of scientific interest within its workspace. In addition to data collected from the Robotic Arm sensors during science support operations, the Robotic Arm will perform experiments along with the other science instruments to yield additional information on Martian soil mechanics in the vicinity of the lander. The experiments include periodic imaging of dumped soil piles, surface scraping and soil chopping experiments, compaction tests, insertion of the various end-effector tools into the soil, and trench cave-in tests. Data from the soil mechanics experiments will yield information on Martian soil properties such as angle of repose, cohesion, bearing strength, and grain size distribution.

1. Introduction

The Mars Volatiles And Climate Surveyor (MVACS) Robotic Arm (see Figure 1) on the Mars Polar Lander (MPL) is a low-mass 4-degree-of-freedom manipulator with a back-hoe design [*Schenker*, 1995]. The end effector (see Figure 2) consists of a scoop for digging and soil sample acquisition, ripper tines for preparing hard soils, secondary blades for scraping, and a Soil Temperature Probe. Control of the arm is achieved by a combination of software executing on the lander computer and firmware resident in the Robotic Arm electronics. Unfortunately the

MPL was lost during descent to the Martian surface on December 3, 1999, so the mission described herein was not conducted.

1.1 Robotic Arm as a support instrument

The MVACS Robotic Arm is an essential instrument in achieving the scientific goals of the MVACS mission by providing support to the other MVACS science instruments as well as conducting arm-specific soil mechanics experiments. One of the primary mission goals is to analyze soil samples in the Thermal Evolved Gas Analyzer. The Robotic Arm will support this goal by acquiring both surface and subsurface soil samples in its scoop from the area in the vicinity of the lander and dumping the soil samples into the TEGA inlet ports. Subsurface soil samples will be acquired at varying depths from within trenches excavated by the arm, potentially to a depth of 50cm depending on the soil conditions (the arm is kinematicaly capable of reaching in excess of one meter below the surface, but operational constraints are expected to limit practical digging depth). To prevent contamination among the samples, the scoop will be cleaned using a specially-designed brush mounted on the lander in between each sample acquisition.

A key element of the MVACS instrument suite is the Robotic Arm Camera (RAC) mounted on the forearm just behind the wrist. Soon after landing the Robotic Arm will position the RAC to take images of the lander foot pads, providing useful data in determining surface properties at the touchdown site. Throughout the mission the arm will periodically position the RAC to take images of the surface, trench floor and end walls, and dumped soil piles. During soil sample acquisition, the scoop will be positioned for the RAC to take close-up images of the soil samples in the scoop prior to delivery to the TEGA. There is a specially-designed divot in the scoop blade to contain small soil samples for very close imaging by the RAC at a distance of 11mm. The arm will also position the RAC for imaging of the magnetic targets located on the TEGA, the scoop cleaning brush, nearby rocks, and any other objects of scientific interest within its workspace.

Further support will be provided to the the 15cm-long Soil Temperature Probe (STP) mounted on the wrist of the Robotic Arm, which will be used to measure surface and subsurface soil temperatures to characterize the soil thermal properties (thermal inertia, conductivity, and diffusivity). The Robotic Arm will position the STP above the surface and then insert the probe into the soil in a sequence of graduated steps. At each step the temperature measurements will be taken along with images by the Robotic Arm Camera. The STP has a graduated scale on it with 1cm increments which will be used as an aid to determine the insertion depth. The Robotic Arm will also position the STP periodically at the surface and subsurface and leave it there for a day at a time to measure surface and subsurface diurnal temperature variations. The Robotic Arm Air Temperature Sensor is the second Metrology (MET) sensor mounted on the Robotic Arm. It will be used to record temperature measurements up to a height of approximately 1.8 meters above the surface and down to within 0.15 meters above the surface depending on the workspace conditions.

1.2 Robotic Arm as a Science Instrument

During the surface operations of the MVACS payload, the Robotic Arm will also be used along with the other MVACS instruments to investigate the physical properties of the surface and subsurface materials in the workspace. The primary surface investigation by the Robotic Arm will be the direct measurements of the mechanical properties using motor currents to determine arm forces. Additional information will be obtained by judicious planning of arm operations, such as purposeful placement of excavated soil to observe the angle of repose and the degradation of the pile due to wind erosion. Other tasks that will be managed as part of the Robotic Arm operations are: grouping and categorization of soil types, tracking and mapping all workspace activities, and archival of all pertinent arm calibration and operations data for future investigations (particularly for areas where real-time analysis will not be feasible during the mission).

Direct measurements by the TEGA of the soil and by the STP of the thermal conductivity will provide additional information useful for understanding the physical properties and chemical composition of the surface and subsurface materials. Much of the information about the soil will come from RAC and the Surface Stereo Imager (SSI). The ability of the RAC to provide close up imaging of material on the tip of the scoop blade at 23micron resolution is an example of how the data gathered by another instrument is highly dependent on cooperative operation with the Robotic Arm - in this case to deliver an appropriate sample to the RAC near focus viewing zone.

The majority of the physical properties experiments will be planned well in advance of the landing of the Mars Polar Lander. This is because previous *in situ* missions have left behind a strong history of materials properties investigations. In particular, the Viking Lander mission investigations [*Moore*, 1987; *Holmberger*, 1980] represent appropriate approaches, which can easily be adapted for use by the MVACS payload. Because of the great similarity in payload capability, it will be possible to provide an easily correlated complementary data set from a region distinct from that of the two Viking missions. Additional information provided by the unique capabilities of the MVACS payload will provide new insights in areas previously not possible.

2. Robotic Arm Description

2.1 Hardware

The MVACS Robotic Arm (see Figure 1) is a 4-degree-of-freedom manipulator with a back-hoe design providing motion about shoulder yaw (azimuth) and shoulder, elbow, and wrist pitch [*Schenker*, 1995]. The arm links are made of a low-mass graphite-epoxy composite. The end effector (see Figure 2) consists of the following tools: a scoop for digging and soil sample acquisition, ripper tines for preparing hard soils, secondary blades for scraping, and the STP. In addition, there are two tools not part of the end effector: the RAC, mounted near the end of the forearm, and the RAATS, mounted above the elbow.

The joint actuators consist of brushed DC motors with 2-stage speed reduction consisting of a planetary gear and harmonic drive (except the wrist, which has a bevel gear at the output of the planetary gear). The actuators are capable of producing 26, 91, 53, and 10 Newton-meters of torque at the joint output during normal operation for joints 1 through 4, respectively. Peak limits are approximately 50% higher. The amount of force that the arm can exert at the end effector is configuration dependent, but is typically around 80 N. Braking is achieved by actively shorting the motor leads to slow the motor until magnetic detents capture the rotor. The detents provide sufficient holding torque to assure no slippage while power is off. Position sensing is accomplished via non-quadrature optical encoders at the motor shaft and potentiometers at the joint output. The encoder counters can be initialized based on potentiometer data or can be set by running each joint up against a known mechanical hardstop located at the end of each joint's travel. The encoder counts are stored in flash memory at the end of each day for use during initialization the following day. Each joint is equipped with an heater (1W for the shoulder and elbow joints and 4W for the wrist joint) and temperature sensor to assure that the motor operation is conducted at or above minimum temperature (208 K). In addition there is a 20W heater for the scoop. See Table 1 for a summary of the Robotic Arm characteristics. The Robotic Arm workspace is depicted in Figure 3.

The RA Electronics (RAE) consists of two PC boards located in the Payload Electronics Box and provides power conditioning; motor voltage control (series pass regulator) and drivers; heater drivers; joint encoder counting; A/D conversion (12 bit) of potentiometer voltages, temperature sensor voltages, motor currents, and total heater current. It also provides interface to the lander Command and Data Handling (C&DH) computer over a 9600 baud serial link. Firmware running on the RAE microprocessor provides for low-level motor command execution to move the joints to the specified positions, heater command execution, A/D calibration, and sensor monitoring. Digital data is updated at 2 ms intervals; analog data is updated at 20 ms intervals.

2.2 Software

The RA flight software resides on the lander Command and Data Handling computer and provides the following functions:

- Initialization (load parameter table and state files, request power on);
- Expansion of high-level task commands;
- Generation of arm movement trajectories;

- Control of arm motion and joint heaters;
- Setting parameters (e.g., motor current limits) in the RAE.
- Reading sensor data and monitoring the arm status;
- Fault detection and recovery;
- Sending arm sensor data to telemetry.

The Robotic Arm has a full suite of arm motion commands that provide for coordinated joint motion as well as Cartesian motion of the end effector [*Taylor*, 1979]. Joint moves can be specified as either absolute moves or relative to the current position. Cartesian moves can be specified as absolute or relative moves with respect to the MVACS coordinate frame located at the base of the Surface Stereo Imager. The operator can also specify Cartesian motion in the local frame of the currently selected tool (scoop blade, STP, tines, secondary blades, or RAC). The four degrees of freedom for Cartesian position are specified as the three translation coordinates plus the angle that the currently selected tool approach vector makes with the plane of the lander deck. Each motion command is broken up into a series of via points that are sent sequentially to the RAE for execution by the firmware. The software control loop sampling period is 200 msec. during which the arm state is monitored for proper operation and the necessary control inputs computed. A block diagram of the control system is given in Figure 4.

The arm can also be commanded to perform more complicated tasks such as digging a trench or acquiring a sample by a single command. The software expands the high-level command into the appropriate set of motion commands which are executed sequentially. This not only saves uplink bandwidth, but eases the burden on the operator in developing complicated command sequences. The software also tracks time and energy resources used during command execution and will gracefully terminate operations when allocations are exceeded. This feature will be most useful when digging a trench due to the uncertainty of the soil properties which affect the execution of the dig trench command.

In addition to providing for control of the free-space arm motions, the software is also capable of executing guarded moves where the arm will move towards its commanded position until contact is made. This is accomplished by monitoring motor currents and computed joint torques versus preset thresholds. Guarded moves will be employed when inserting the STP into the ground, acquiring samples, and when digging trenches. Thus, Robotic Arm operation is robust with respect to surface location uncertainty.

To aid in safety and increase autonomy, the Robotic Arm software is capable of detecting and recovering from faults and anomalous events. Faults and events are defined as follows:

- Fault - inability to complete a command due to failure of hardware (sensor, actuator, electronics, etc.) or software;
- Event - inability to complete a command due to anything other than a fault (e.g., arm motion impeded due to hard soil).

If a fault or event is detected, the fault or event type is reported in telemetry. Depending on the fault or event detected, the RA software will either attempt to recover from the fault or event or place the arm in a safe configuration. It is expected that the Robotic Arm will occasionally encounter conditions that impede its motion during digging (a rock in the soil, a patch of ice, etc.). The software has a built-in accommodation algorithm, similar to [*Bonitz*, 1996], to compensate for this condition by adjusting the scoop trajectory and, if necessary, dumping the scoop contents and re-executing the digging motion.

The primary operations tool for commanding the Mars '01 Robot Arm will be the Web Interface for Telescience (WITS) system [*Backes*, 2000]. WITS provides target designation from panorama image data, generates command subsequences via programmed macros, simulates arm motion, checks for collisions, computes resources (energy, time, data), and outputs a complete command sequence file for uplink to the Lander.

3. Development Testing and Calibration

The Robotic Arm was extensively tested during development to verify that the design could withstand the harsh environmental conditions expected as well as to characterize the performance of the actuators and to calibrate the sensors and kinematic model of the arm. Qualification testing included both vibration to simulate launch loads and thermal-vacuum testing to simulate the Martian environment (temperature and pressure).

The performance of the actuators were evaluated over a temperature range of 183 K to 293 K and expected operating voltages. Data from the characterization are used by the control system to continuously monitor joint torques for use in executing guarded moves, in the accommodation algorithm and to prevent excessive torque from damaging to the joints. The joint output torques are computed by first computing the no-load motor currents which are both temperature and voltage dependent and then computing the torque from the actuator torque constant. The no-load motor currents are computed from

$$I_{nl} = I_o + ae^{-bT}(V/V_{max})$$

and the joint torques from

$$\tau = K_a(I - I_{nl})$$

where I_{nl} is the no-load motor current, I_o is the no-load motor current at 293 K, a and b are constants, T is the temperature, V is the applied motor voltage, V_{max} is the maximum operating voltage, τ is the torque, I is the motor current, and K_a is the actuator torque constant. The constants a, b, and I_o were determined from the test data by using a least-squares fit. No-load motor currents are plotted in Figure 5 with key actuator parameters given in Table 3. During the landed mission, a standard set of free-space moves will be periodically executed to monitor actuator performance. In addition, the joint heaters will be operated to characterize the thermal properties of the joints in the Martian environment.

Calibration of the arm position sensors and kinematic model was done moving the arm through a series of poses throughout the workspace and measuring the location of the end effector using a system of highly accurate theodolites. The sensor and kinematic model parameters were then determined by solving a constrained minimization problem that minimizes the mean error over the measured poses. The kinematic model parameters are based on the method of Denavit and Hartenberg [*Denavit*, 1955]. Robotic Arm frame assignments are shown in Figure 6. The position of all joints in Figure 6 is zero degrees. See Figure 3 for a definition of zero degrees in azimuth with the Robotic Arm mounted on the lander. Positive joint rotations are clockwise about the z axes using the right-hand rule. Kinematic parameter values are given in Table 4. Frame assignments for the end-effector tools are shown in Figure 7 and the location of each tool frame in wrist-frame coordinates is given in Table 5. The angle, θ, is the angle from wrist-frame z axis to the tool-frame z axis about the wrist-frame y axis.

Sensor parameters are given in Table 6. Sensor offsets are the outputs of the A/D converter when the corresponding parameter being measured (angle, temperature, or current) is zero. E.g., when the joint 1 reading is 1494, the joint 1 angle is zero degrees. The encoder slopes are given with respect the joint output angle, not the motor shaft angle.

During digging and soil-mechanics experiments, estimates of forces exerted by the end-effector tools are important data for use in determining soil properties. These estimates can be made from the sensed motor currents, but will be somewhat crude due to unmodeled arm dynamics and the limited degrees of freedom of the arm. During digging and soil mechanics experiments, reaction from the soil can exert forces on the end effector which cannot be detected at the arm joints via the sensed motor currents due to the limited degrees of freedom and the fact that all of the motors are not on at all times during arm motion. End-effector forces can be estimated from

$$F_e = J^{T\#}\tau$$

where F_e is the force vector exerted by the end effector, $J^{T\#}$ is the pseudoinverse of the manipulator Jacobian [*Spong*, 1989] transpose with the rows associated with the unactuated joints removed, and τ is the vector of joint torques for the actuated joints. End-effector forces in the null space of J^T will not appear in the joint torques. The manipulator Jacobian is dependent on arm configuration and, thus, the transformation to end-effector forces and the null space changes as the joint angles change.

Along with the calibration and qualification testing, additional digging tests were performed in the lab and in the field. Laboratory work concentrated primarily on the development of the end-effector tools, though limited digging tests were also possible in support of software development. Much of the early design work on the Robotic Arm end effector was inspired by discussions at the Mars soil science workshop held at NASA Ames in 1996. At the workshop scientists with field experience in the Antarctic Dry Valleys, which have similar thermal and hydrologic conditions as are expected on Mars, provided a number of valuable insights into how to dig in frozen soils. Additionally, two MVACS team members and a National Science Foundation guide tested the ability of the robotic arm end effector to dig trenches at a variety of Antarctic Dry Valley sites (see Figure 8). This effort was focused on learning how to use the Robotic Arm to perform the same soil handling operations planned for use on Mars.

An example of one of the techniques tested with the manual digging tool is the re-surfacing of the end of a rough trench to obtain a smooth fresh surface for photo documentation. Iain Campbell from New Zealand has demonstrated that by carefully shaving the vertical walls of a trench in the dry valleys he has been able to photograph the layering in the soil clearly enough to make some important findings relating to volatile movement and saltation [*Campbell*, 1998]. Using the RAC and this technique, we expect to be able to discern the fine scale layering expected at the Mars Polar Lander landing site. An example of this type of image can be found in Figure 9, which shows a trench dug using an end effector mockup. Additional trench excavation experience was gained relating, for example, to the minimum trench width to allow sample acquisition without disturbing the trench wall (to maintain sample depth uniformity).

4. Experimental Investigations

Data acquired as part of the physical properties experiments will come from many sources. A majority of the RA operations will be in support of the primary mission objectives including: digging, dumping, acquiring samples, STP insertion, and scoop cleaning. Although these activities will not be performed specifically to provide materials properties data, by tailoring the operational sequences carefully it will be possible to leverage this data with that from other instruments to gain additional insight. For example, by maintaining a constant dump location for a few hours of operation while digging a trench, a rather sizable conical pile can be obtained. In order for this pile to be useful for observing changes over time, it should be in an isolated area, which necessitates moving the dump location for future digging to another area. This means extra effort in managing the available workspace as a resource, as well as the additional wear on the actuators for the additional movement, but the supplementary data necessitates the effort. Another example of tailoring operations to maximize data content is the choice of the angle to dig the trench. There is only one azimuth angle that allows the SSI to image directly down the length of the trench (see Figure 3). In order to optimize viewing by the SSI, primary trenching operations will be performed at this digging angle if surface conditions.

Another science tradeoff made on a daily basis will be the amount of digging data that is sent back to earth. Due to resource limitations of the lander, it may be necessary to decrease the data collection rate for the arm in order to obtain extra imaging or MET data. These decisions will be made based on the relative value of the data as determined by the science team, and will be heavily influenced by the relative quality of the data sets and their contribution to the overall mission goals. An example would be if the soil is particularly soft and uniform, then extra images would be more useful than than digging data collected at a high sample rate for determining soil characteristics.

In addition to the data gained during regular arm operations, specific materials properties experiments will be performed (see Table 7). Because of the criticality of the efficient operation of the arm to support the rest of the science objectives (particularly acquiring samples for the

TEGA) , dedicated materials properties experiments will be done based on available resources. However, even under adverse conditions it should be possible to perform a substantial number of dedicated experiments. The following is a partial list of some of the physical properties experiments that will be conducted:

a) **STP and scoop blade insertion to determine soil penetration resistance**. The shape of the STP is quite similar to that of a standard conical soil penetrometer, though the small diameter of the STP limits the range of soil types that it can be used in. For softer materials the leading edge scoop blade will be used to approximate the insertion of a two-dimensional plane to obtain similar data.

b) **Scraping with the scoop blade, the secondary blades, and the ripper tines**. The cutting ability of the different cutting tools will yield information on the cohesion of the soil. Close-up imaging of wear on the scoop blade will provide grain strength data. If the opportunity is presented, rocks within the workspace will be abraded using the tools on the scoop.

c) **Intentionally causing the trench to cave in.** By under-cutting the wall of the trench or by using the under side of the scoop to apply pressure at the surface next to the edge of the wall it will be possible to cause a trench wall to cave in under controlled conditions, yielding bearing strength data.

d) **Chopping soil samples.** The ability of the arm to repeatedly chop a sample in preparation for TEGA delivery will provide cohesion data. This capability can be used with any of the end-effector tools, including the STP, allowing for many possible experiments.

e) **Shaking the end effector and brush.** Because of the flexibility and length of the arm it is possible to create repeatable agitations to shake loose particles, allowing for insight into particle adhesion. The brush is also mounted to a flexible member to allow the arm to clean particles from the bristles by pulling upward on the brush with the end of the scoop blade until the brush slips off the end of the blade. This brush "twang" procedure imparts significant vibrations to both the brush and the arm.

f) **Excavated soil piles.** Long term data will be gathered by monitoring the evolution of purposefully placed conical excavated soil piles. Along with angle of repose and wind erosion, the piles are expected to be a likely site for frost formation early in the mission.

5. Data Products

The Robotic Arm subsystem generates two kinds of telemetry - engineering and science. Engineering telemetry consists of current arm state data that is downlinked at the completion of each Robotic Arm command. Science telemetry consists of detailed sensor data collected every 200 milliseconds during command execution. Robotic Arm science telemetry is used for reconstruction of the digging process, soil-mechanics experiments and for trouble shooting.

The following engineering data is reported to the telemetry system at the completion of each Robotic Arm command (except where noted):

- Command op code;
- Joint position from encoders (radians);
- Joint position from potentionmeters (radians);

- Joint temperatures (degrees Celsius);
- Sum of heater currents (amps, reported upon change);
- Energy consumed (watt-hours);
- Voltage references (volts);
- Health status (reported upon fault or event)

While the arm is moving, raw arm sensor data is collected every 200 milliseconds and stored for subsequent downlink in telemetry. All analog data is converted to 12-bit digital format. The following raw digitized data is collected:

- Joint angle encoder count;
- Joint angle potentiometer voltage;
- Joint temperatures;
- Motor currents;
- Motor voltages;
- Status word (motor, brakes, and heater state information);
- Sum of heater currents;
- Time - 12 msec. resolution.

The Robotic Arm science telemetry will be the most useful for scientific analysis of soil properties during digging and soil-mechanics experiments. The motor currents along with the reconstructed arm trajectories will yield information regarding the degree of difficulty of digging in the various soils encountered and of executing the arm motions during the various soil-mechanics experiments. In addition to the data listed above, detailed history of the arm state and control variables for the last one minute of operation is downlinked whenever a fault or event occurs. This will permit reconstruction of the exact sequence of events leading to the anomaly.

The following data will be archived in the Planetary Data System (http://pds.jpl.nasa.gov) for use by the science community:

- Position data for the STP, RAC, and elbow temperature sensor;
- Joint positions, temperatures and motor currents for reconstruction of arm trajectories and joint torques;
- Calibration report;
- Experimenter's notebook.

6. Conclusion

The MVACS Robotic Arm is an essential element in carrying out the MVACS science experiments. In support of the other instruments, it will dig trenches in the Martian soil, deliver soil samples to the TEGA, and position the STP and the RAC. The Robotic Arm will also conduct arm-specific science experiments to collect data relating to soil properties such as periodic imaging of dumped soil piles, surface scraping and soil chopping experiments, compaction tests, insertion of the various end-effector tools into the soil, scoop shake tests and trench cave-in tests. Key data elements include joint motor currents and trajectories which will be used to estimate end-effector forces during arm operations. Data from the Robotic Arm support operations and science experiments when combined with data from the other instruments will yield important information on Martian soil properties, providing valuable insight into the history of Mars.

Acknowledgements

The research described in this paper was carried out by the Jet Propulsion Laboratory, California Institute of Technology, under a contract with the National Aeronautic and Space Administration. We would also like to thank the following for their support throughout the development of the MVACS Robotic Arm: Young Park, Barry Goldstein, Nancy Marmor, Jim McGown, Steve Bailey, and the Lockheed Martin team.

References

Bonitz, R. G., and T.C. Hsia, Robust internal force-tracking impedance control for coordinated multi-arm manipulation - theory and experiments, *Proceedings of the 6th International Symposium of Robotics and Manufacturing*, 2nd World Automation Congress, Montpellier, France, May 1996

Backes, P. G., K. S. Tso, J. S. Norris, G. K. Tharp, J. T. Slostad, and R. G. Bonitz, Mars Polar Lander mission distributed operations, in *Proceedings IEEE Aerospace Conference*, Big Sky, Montana, March, 2000

Denavit, J. and R. S. Hartenberg, A kinematic notation for lower pair mechanisms, *J. Applied Mechanics*, Vol. 22, pp. 215-221, 1955

Holmberger, N. A., R. P. Faust, and H. M. Holt, Viking '75 spacecraft design and test, *Summary Volume 1, NASA Reference Publication 1027*, pp. 174-180, 1980

Moore, H. J., R. E. Hutton, G. D. Clow, and G. E. Spitzer, Physical properties of the surface materials at the Viking landing sites on Mars, *U.S. Geological Survey Professional Paper 1389*, 1987

Schenker, P. S., D. L. Blaney, D. K. Brown, Y. Bar-Cohen, S-S. Lih, R. A. Lindemann, E. D. Paljug, J. T. Slostad, G. K. Tharp, C. E. Tucker, C. J. Voorhees, C. Weisbin, E. T. Baumgartner, R. B. Singer, and R. Reid, Mars lander robotics and machine vision capabilities for in situ planetary science, in *Intelligent Robots and Computer Vision XIV, SPIE Proc. 2588*, Philadelphia, PA, October, 1995.

Spong, M. W. and M. Vidyasagar, *Robot Dynamics and Control*, John Wiley and Sons, pp. 111-119, 1989

Taylor, R., Planning and execution of straight-line manipulator trajectories, *IBM Journal of Research and Development*, Vol. 23, No. 4, pp. 424-436, 1979

Campbell, I. B., G. G. C. Claridge, D. I. Campbell, and M. R. Balks, The soil environment of the McMurdo Dry Valleys, Antarctica, in *Ecosystem Dynamics in a Polar Desert, The McMurdo Dry Valleys, Antarctica*, edited by J. C. Priscu, pp. 297-322, American Geophysical Union, Washington, D. C., 1998

Figure 1 MVACS Robotic Arm

Figure 2 Robotic Arm End Effector

Figure 3 Robotic Arm Workspace

Figure 4 Robotic Arm Controller

Figure 5 No-load Motor Currents

Figure 6 Robotic Arm Frame Assignments

Figure 7 Tool Frame Assignments

Figure 8 Digging Tests in Antarctica

Figure 9 Trench Side Wall

Table 1 Robotic Arm Parameters

Parameter	Value	Comment
Degrees of freedom	4 rotary joints - shoulder yaw (azimuth), shoulder pitch, elbow pitch, wrist pitch.	Back-hoe design.
Reach	2.2 m	
Max Cartesian velocity	0.07m/sec	Configuration dependent.
Mass	5 Kg.	Includes electronics (868g).
Materials:		
Upper arm and forearm link	Graphite-epoxy tubes.	
Scoop Blade	6Al-4V Ti STA	
Secondary Blades	Tungsten Carbide, GC015	
Ripper Tines	6Al-4V Ti STA	
Actuators	Brush DC motors with 2-stage drive train (planetary gear plus harmonic drive).	Wrist has bevel gear for 2nd stage instead of harmonic drive.
Accuracy and repeatability	1 cm and 0.5 cm, respectively.	
End-effector force capability	Configuration dependent; typically 80 Newtons.	

Table 2 Robotic Arm Joint Parameters

Parameter	Joint 1	Joint 2	Joint 3	Joint 4	Units
Actuator output torque	26	91	53	10	Newton-meters
Gear ratios	12500	16000	10000	4000	
Min angle	-89	-138	-27	0	degrees
Max angle	196	80	231	217	degrees
Max speed (no load)	2.0	1.5	2.5	6.1	deg/sec
Heaters	1	1	1	4	watts

Table 3 Actuator Parameters

Parameter	Joint 1	Joint 2	Joint 3	Joint 4	Units
Torque constant	442	448	332	95.5	N-m/A
I_o	0.020	0.024	0.020	0.013	A
a	0.0002	0.0020	0.0015	0.0036	A
b	0.0684	0.0530	0.0538	0.0079	1/K
V_{max}	30	30	30	30	Volts

Table 4 D-H Parameters

Link	Length, *a*, in meters	Offset, *d*, in meters	Twist, α, in degrees
1	0.0276	0.0553	-90
2	1.0007	-0.13575	0.0
3	0.9564	0.0	0.0
4	0.0	0.0	90

Table 5 Tool Kinematic Parameters

Tool	x in meters	y in meters	z in meters	θ in degrees
Secondary Blade 1 (front)	-0.0365	0.0	0.1088	61.9
Secondary Blade 2 (rear)	-0.0593	0.0	0.1014	-98.1
RAC	-0.1455	-0.0047	-0.0646	99.9
Scoop (blade tip)	0.0782	0.0	0.1325	74.1
STP	0.1469	-0.0319	-0.0983	123.8
Tines 1 (front)	-0.0826	0.0	0.0828	27.9
Tines 2 (back)	-0.0879	0.0	0.0729	-152.1

Table 6 Sensor Parameters

Parameter	Joint 1	Joint 2	Joint 3	Joint 4	Units
Pot offset	1494	1996	1048	634	bits
Pot slope[†]	0.0833	0.0835	0.0834	0.0846	degrees/bit
Encoder offset	7187	13248	2484	991	bits
Encoder slope	0.0144	0.0112	0.0180	0.0450	degrees/bit
Temperature sensor offset	1944	1943	1939	1936	bits
Temperature sensor slope	0.225	0.225	0.225	0.225	degrees K/bit
Motor current sensor offset	2048	2048	2048	2048	bits
Motor current sensor slope	0.375	0.375	0.375	0.375	mA/bit

[†] Approximately constant over operating temperature range.

Table 7 Soil Properties

Property	Task
Adhesion	Imaging of scoop, brush, and lander
Angle of internal friction	Surface bearing tests using bottom of scoop, imaging footpads
Angle of repose	Imaging of natural slopes, trench walls, tailing piles.
Bearing Strength, Cohesion	Imaging of footpads and trench wall
Bulk Density	Imaging of footpads
Chemical Compositions	TEGA analysis
Grain size distribution	RAC imaging and TEGA sorting on screen before and after vibration.
Grain strength	
Heterogeneity	RAC imaging, arm forces while digging, STP insertion
Magnetic Properties	TEGA magnets and SSI target plate magnets
Penetration resistance	Scoop Blade, Scoop Bottom, and STP insertion
Thermal Conductivity and Inertia	STP use

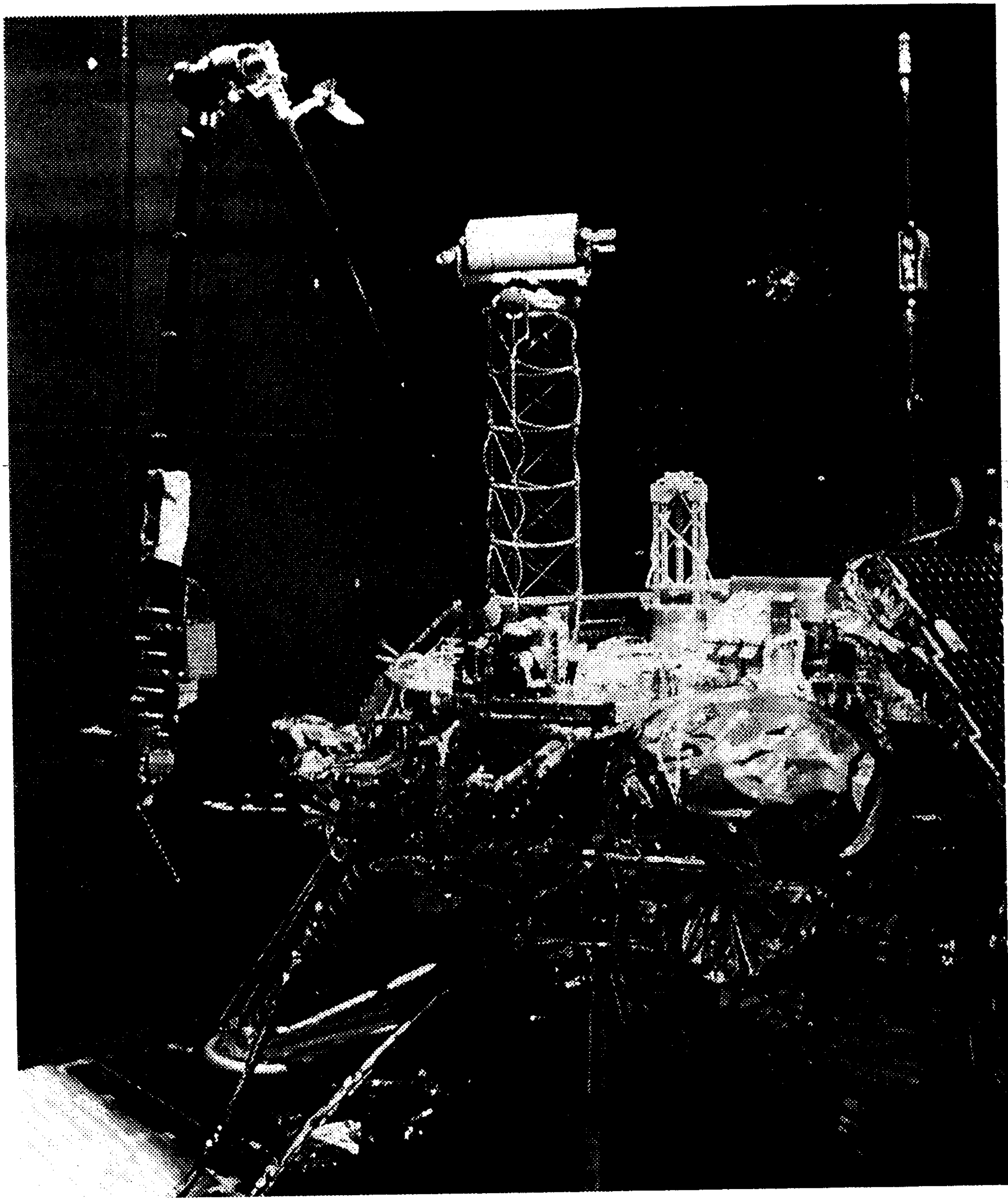

1

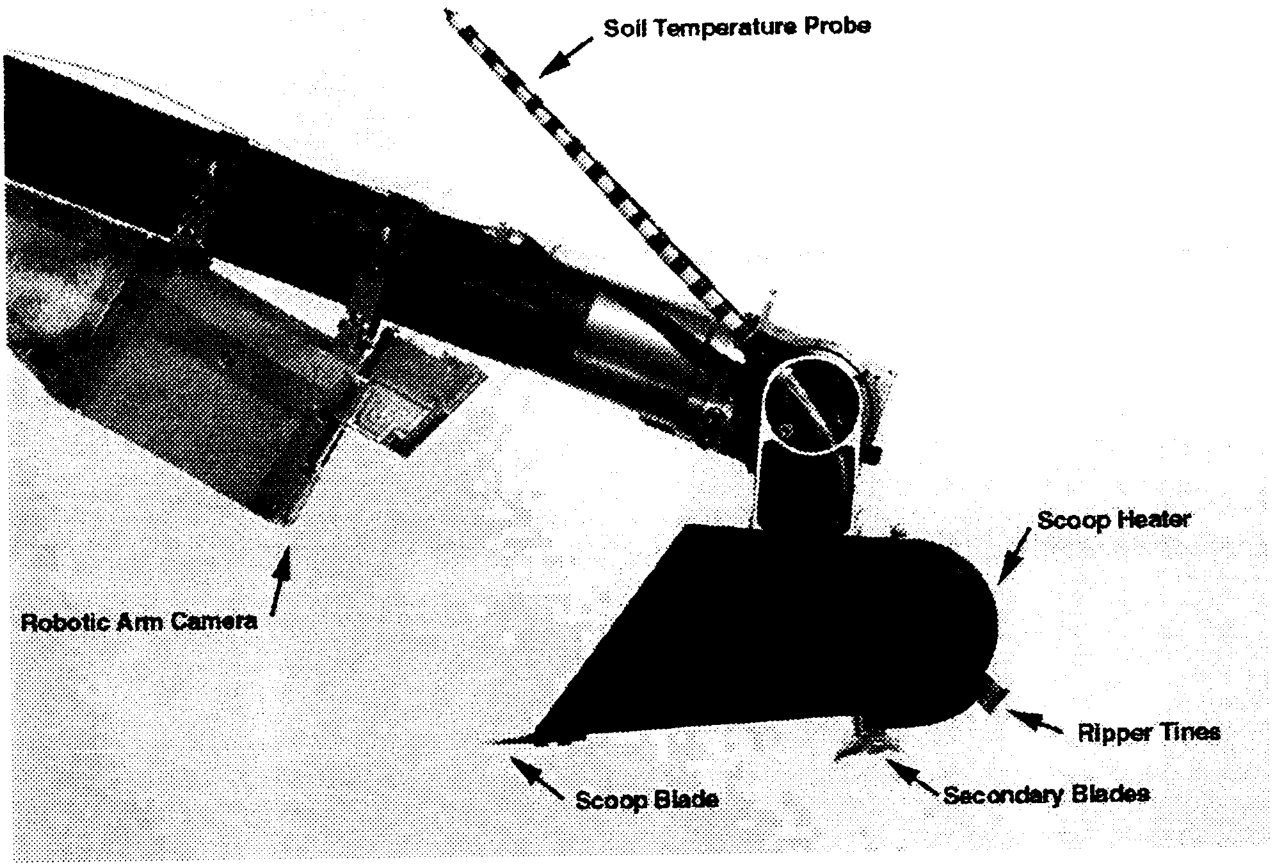
Soil Temperature Probe
Robotic Arm Camera
Scoop Heater
Ripper Tines
Scoop Blade
Secondary Blades

2

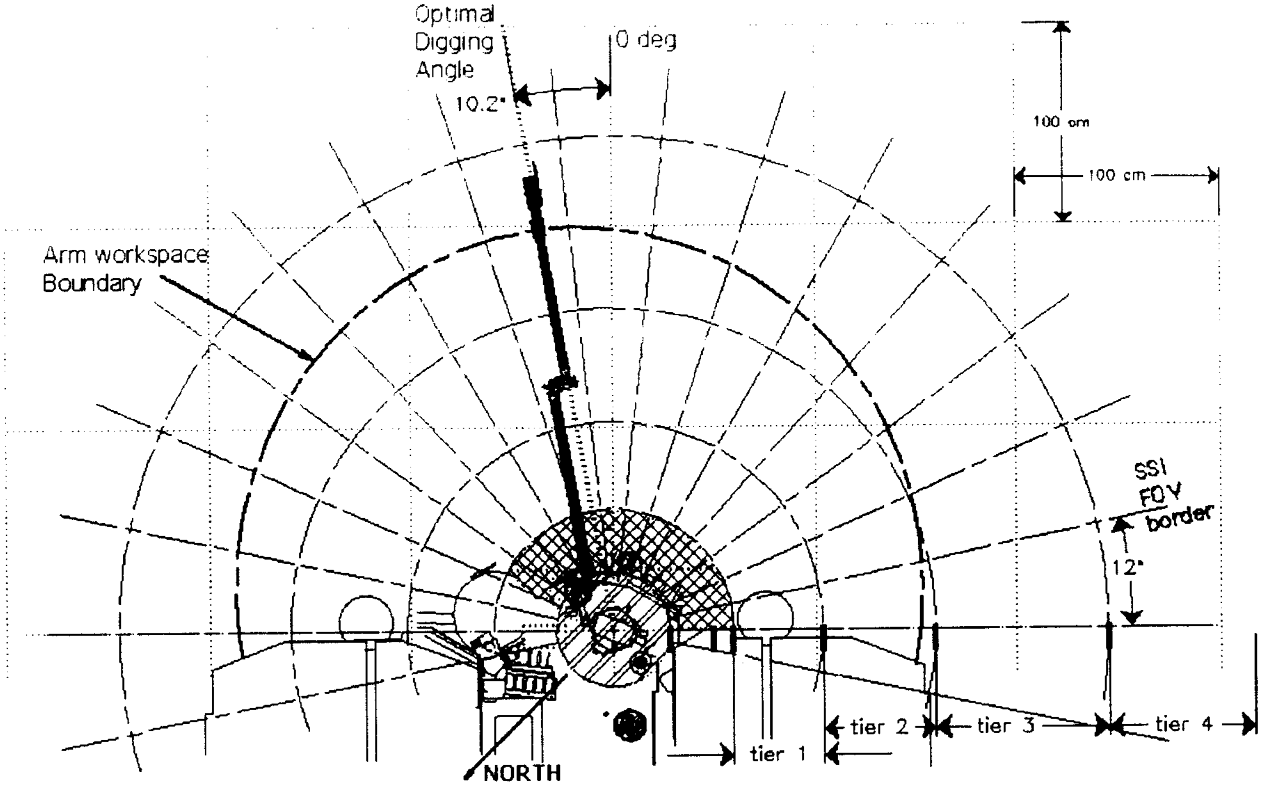
Optimal
Digging
Angle
0 deg
10.2°
100 cm
100 cm
Arm workspace
Boundary
SSI
FOV
border
12°
tier 2
tier 3
tier 4
tier 1
NORTH

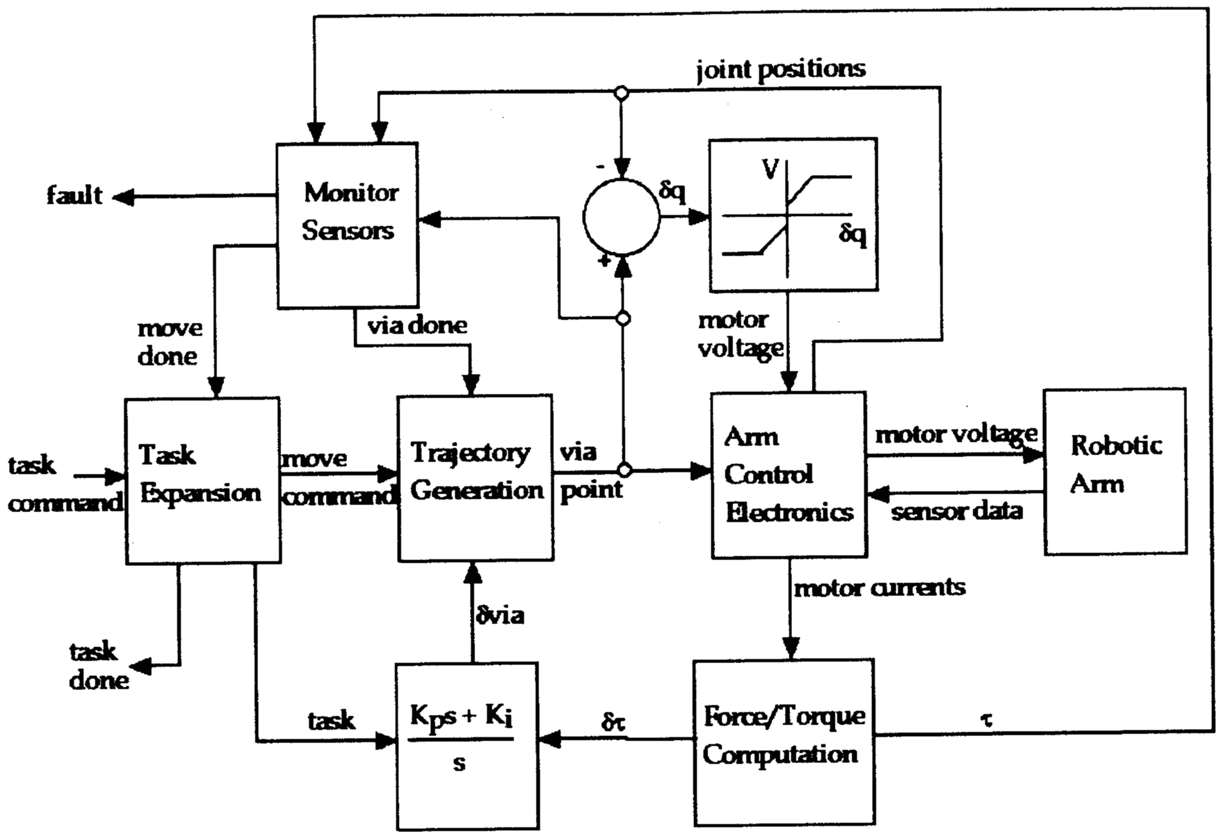
joint positions
Monitor Sensors
fault
δq
V
δq
move done
via done
motor voltage
task command
Task Expansion
move command
Trajectory Generation
via point
Arm Control Electronics
motor voltage
Robotic Arm
sensor data
motor currents
δvia
task done
task
Kps + Ki
s
δτ
Force/Torque Computation
τ

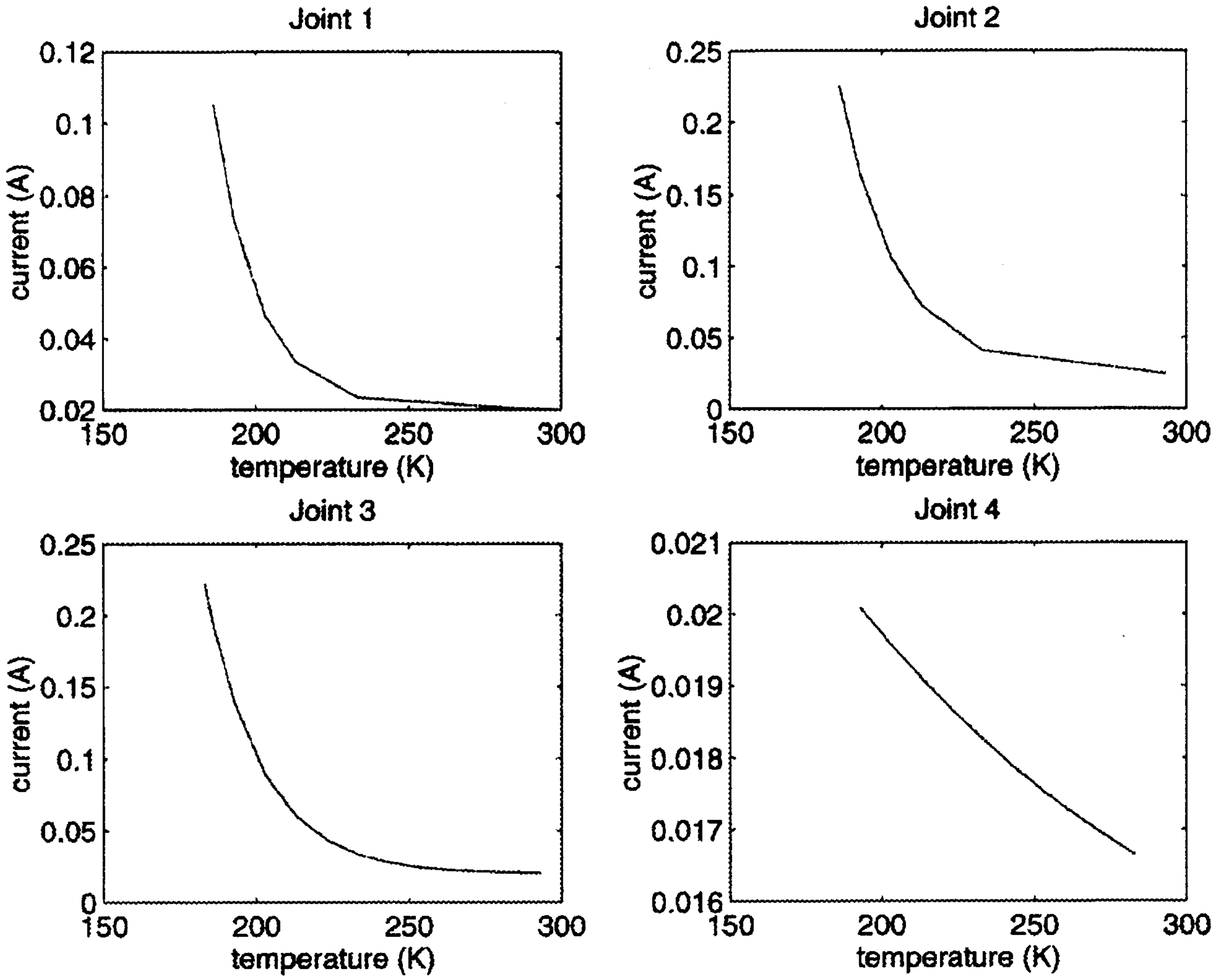
Joint 1
0.12
0.1
0.08
0.06
0.04
0.02
current (A)
150
200
250
300
temperature (K)
Joint 2
0.25
0.2
0.15
0.1
0.05
0
current (A)
150
200
250
300
temperature (K)
Joint 3
0.25
0.2
0.15
0.1
0.05
0
current (A)
150
200
250
300
temperature (K)
Joint 4
0.021
0.02
0.019
0.018
0.017
0.016
current (A)
150
200
250
300
temperature (K)

5

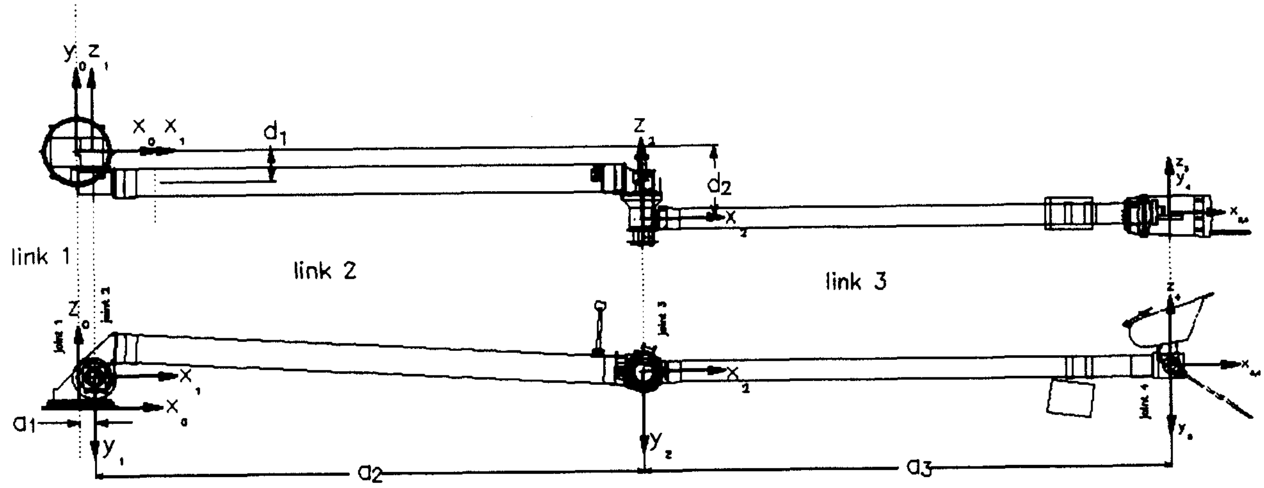

link 1
link 2
link 3
d1
d2
a1
a2
a3

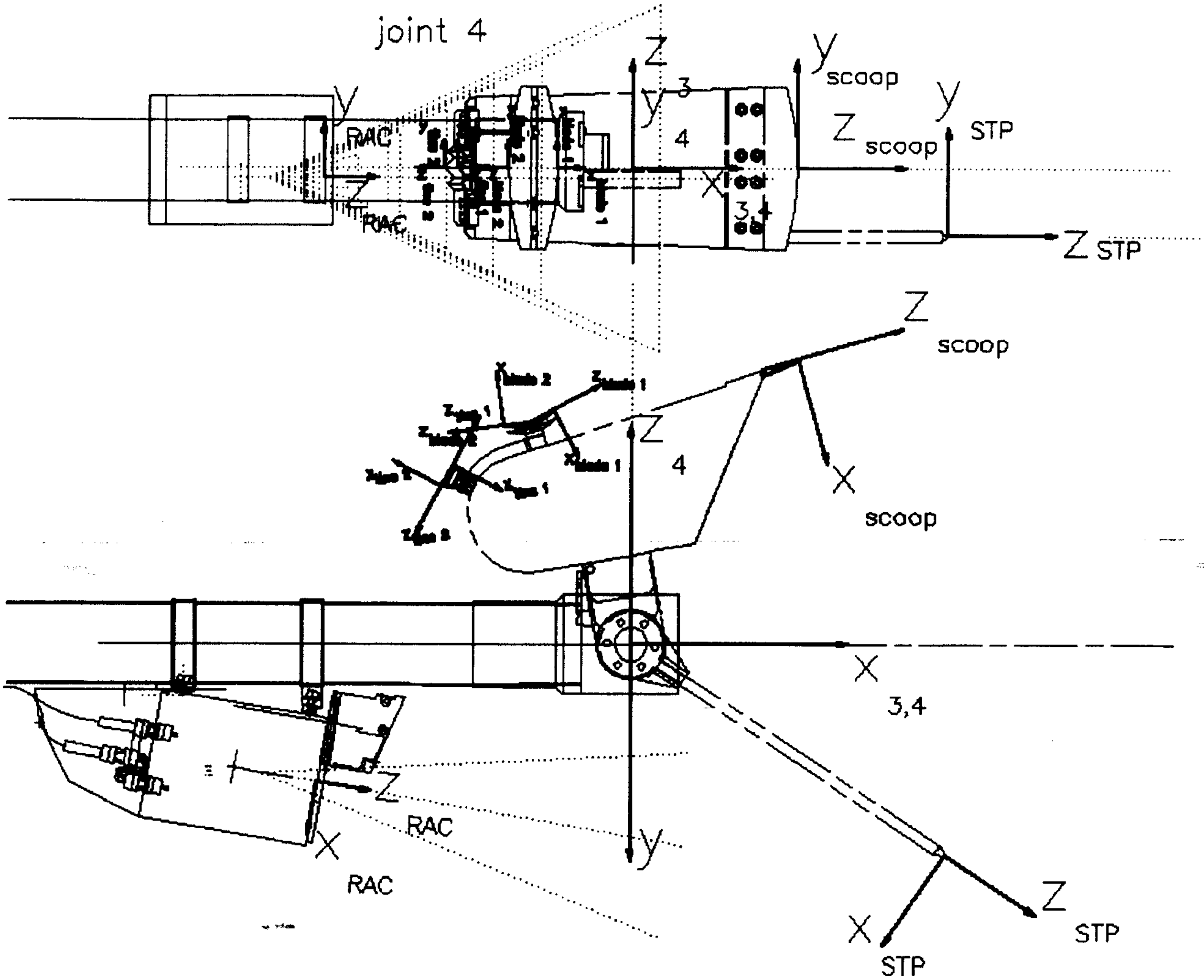
joint 4
y
RAC
Z
RAC
Z
y 3
4
X
3,4
y
scoop
Z
scoop
y
STP
Z STP
Z
scoop
Z
4
X
scoop
X
3,4
Z
RAC
X
RAC
y
Z
STP
X
STP

8